

Initiating and Monitoring the Evolution of Single Electrons Within Atom-Defined Structures

Mohammad Rashidi,^{1,2,3,*} Wyatt Vine,^{1,†} Thomas Dienel,^{1,2,‡} Lucian Livadaru,³ Jacob Retallick,⁴
Taleana Huff,^{1,3} Konrad Walus,⁴ and Robert A. Wolkow^{1,2,3}

¹*Department of Physics, University of Alberta, Edmonton, Alberta, T6G 2J1, Canada*

²*Nanotechnology Initiative, Edmonton, AB, Canada, T6G 2M9*

³*Quantum Silicon, Edmonton, AB, Canada, T6G 2M9*

⁴*Department of Electrical and Computer Engineering, University of British Columbia, Vancouver, BC, V6T 1Z4, Canada*



(Received 21 November 2017; revised manuscript received 24 July 2018; published 15 October 2018)

Using a noncontact atomic force microscope, we track and manipulate the position of single electrons confined to atomic structures engineered from silicon dangling bonds on the hydrogen terminated silicon surface. An attractive tip surface interaction mechanically manipulates the equilibrium position of a surface silicon atom, causing rehybridization that stabilizes a negative charge at the dangling bond. This is applied to controllably switch the charge state of individual dangling bonds. Because this mechanism is based on short range interactions and can be performed without applied bias voltage, we maintain both site-specific selectivity and single-electron control. We extract the short range forces involved with this mechanism by subtracting the long range forces acquired on a dimer vacancy site. As a result of relaxation of the silicon lattice to accommodate negatively charged dangling bonds, we observe charge configurations of dangling bond structures that remain stable for many seconds at 4.5 K. Subsequently, we use charge manipulation to directly prepare the ground state and metastable charge configurations of dangling bond structures composed of up to six atoms.

DOI: 10.1103/PhysRevLett.121.166801

Atomic manipulation [1,2] has emerged as a powerful strategy to fabricate novel atomic physical-systems [3–5] and devices [6–9]. An important addition to this experimental toolkit would be the ability to design and control functional atomic charge configurations with single electron precision. To this end, several studies have demonstrated the ability to create, move, and controllably switch single charged species on a surface with scanning probe techniques [10–20]. One commonality of prior charge manipulation studies is that they have relied upon the application of bias voltage to induce charge transitions. In most cases, this results in a non-negligible tunneling current, whereas in principle, charge manipulation could be performed by transferring single electrons. Two recent works highlight progress in this area: Steurer *et al.* [16] have demonstrated the lateral manipulation of charge between pentacene molecules adsorbed to a NaCl thin film and Fatayer *et al.* [20] have performed charge manipulation with zA tunneling currents. One drawback of these approaches, however, is that in order to limit the tunneling current, a large tip-sample separation was required (up to several nm), thereby sacrificing spatial resolution.

Building on these efforts, we present the manipulation of charge within nanostructures engineered from silicon dangling bonds (DBs) on a hydrogen-terminated Si(100)-(2 × 1) surface. One advantage to working with DBs is that because they are midgap states, they are electronically isolated from

the bulk substrate [21]. DBs can therefore localize charge without the requirement of a thin insulating film between structure and substrate, which has been essential in many previous studies [10–16,20,22,23]. Recent advances in the patterning of DBs have made it possible to create large error-free structures [24–26]. Noncontact atomic force microscopy measurements [27] have confirmed that the energy of the neutral to negative (0/−) charge transition of an isolated DB on a highly *n*-doped sample is close to the bulk Fermi level (within a few hundred meV). This enables the charge state of DBs to be selectively modified by shifting the (0/−) charge transition level above or below the bulk Fermi level with bias voltage or other nearby charged DBs [9,21,27,28]. In contrast, here we demonstrate charge state control of DBs based on a mechanical mechanism; the probe is used to manipulate the equilibrium position of the DB's host atom, making it energetically favorable to host a negative charge. Because this ability is based on short range interactions between the probe and target atom, and can be performed with zero applied bias voltage (0 V), close proximity to the sample is maintained, ensuring both site-specific selectivity and single-electron control.

Figure 1(a) displays two DBs patterned with two intervening hydrogen atoms using voltage pulses applied to the probe [29]. Pairs of DBs are known to host only a single negative charge because the Coulombic repulsion between

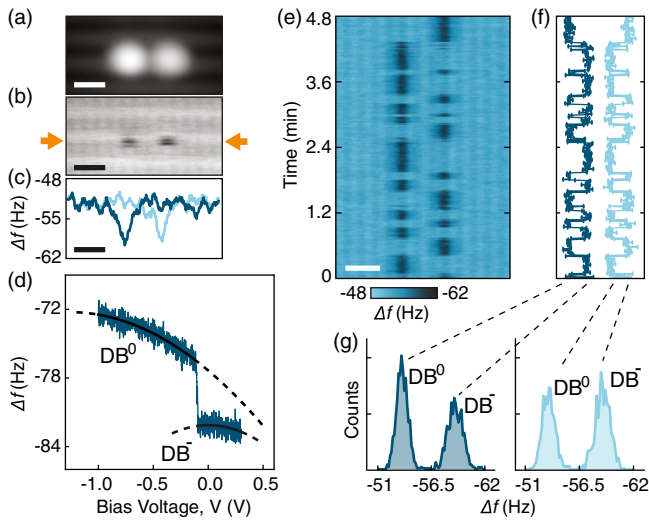


FIG. 1. Charge configurations of two closely-spaced DBs. (a) Constant current filled state STM image, -1.8 V, 50 pA. (b) Constant height Δf image, 0 V, -300 pm. (c) Two constant height Δf line scans (0 V, -300 pm) at the position indicated by the orange arrows in (b). (d) $\Delta f(V)$ spectroscopy taken above an isolated DB (-370 pm). The two individual segments have been fitted by two parabolas (solid lines: fit, dashed lines: extrapolation) corresponding to the neutral and negatively charged states (DB^0 and DB^- , respectively). (e) Combined map of 400 constant height Δf line scans (0 V, -300 pm) taken sequentially over a 4.8 minute period. (f) Time-dependent bistable signal for the two individual DBs extracted from (e). (g) Histograms of the signals in (e). Labels indicate the charge state assignment of each peak. Scale bar is 1 nm (a)–(c),(e).

two closely-spaced negative charges would otherwise be too large [21]. Here, constant height frequency shift (Δf) images of the pair appear streaky because the negative charge switches sites multiple times over the time it took to acquire an image [Fig. 1(b)]. This is seen clearly in individual Δf line scans across the structure [Fig. 1(c)] that reveal the localization of charge to one DB, with subsequent line scans demonstrating that this charge occasionally switches to the other DB. To definitively assign the contrast observed over each DB in Δf images to a charge state, we performed bias-dependent Δf spectroscopy [$\Delta f(V)$] on an isolated DB [Fig. 1(d)], which is negatively charged at 0 V on highly n -doped samples [27,29]. Figure 1(d) reveals a sharp transition between two parabolas [12], associated with switching between the neutral (left of the step) and negatively charged states of the DB. Comparing the Δf of the negatively charged state measured at 0 V to the extrapolation of the neutral state's parabola at 0 V confirms that the dark contrast (larger $|\Delta f|$) in Figs. 1(b),1(c) correspond to the negatively charged DB.

By stacking sequential Δf line scans [Fig. 1(f)], we monitored the charge switching between the two sites in real time. Previous theoretical estimates for the tunneling rate between two closely-spaced DBs have ranged from THz to GHz, depending on the spacing [41,42]. Surprisingly, the

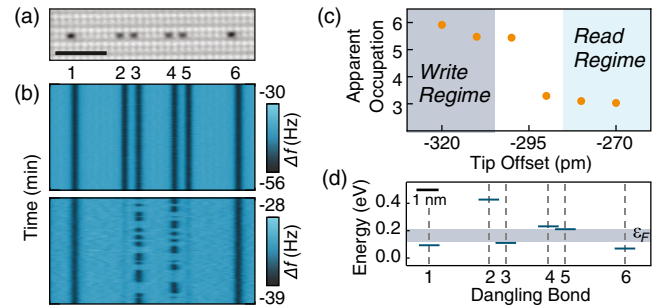


FIG. 2. Evolution of charge configurations of a symmetric six DB structure at different tip heights. (a) Constant height Δf image (0 V, -300 pm). (b) Maps of 800 constant height Δf line scans acquired over 18 minutes at -320 pm (top panel) and -270 pm (bottom panel). The scale bar in (a) is 3 nm and applies to (b). Color bars correspond to Δf . Histograms of the Δf extracted over each DB in (b) are available in Supplemental Material, Fig. S(3) [29]. (c) The average occupation of the structure inferred from digitizing the charge configuration at different Δz . Two interaction regimes: *read* and *write* are indicated. (d) Energetic shift of the $(0/-)$ levels of each DB in the structure (1, 3, and 6 are negatively charged) with respect to the $(0/-)$ level of an isolated DB (0 eV). The levels are shifted Coulombically by the negative charges confined to the structure and are calculated in the absence of the probe using an electrostatic approximation of point charges and a surface dielectric constant of 6.35 . Because the exact energy of the $(0/-)$ level is unknown, we indicate a range of energies (blue shaded area) over which the bulk Fermi level would give rise to the charge configurations observed in the lower panel of (b).

bistable signal for each DB extracted from Fig. 1(f) demonstrates that the system's charge configuration often remains stable for seconds [Fig. 1(g)]. Recent studies have revealed that charged species are often stabilized by a lattice relaxation of the supporting substrate [10,20,43]. Density functional theory has similarly shown that negatively charged silicon DBs experience approximately 200 meV stabilization due to a relaxation of the lattice, which results in the nuclear position of the host atom being raised by approximately 30 pm relative to the neutral state [44–46]. In this case, the lattice relaxation prevents the electron from elastically tunneling between the paired DBs. To assign the position of the charge in each Δf line scan, each trace was fitted with two Gaussian profiles. Histograms of the determined Δf center values demonstrate two Gaussian profiles, representing the negative and neutral charge states of each DB [Fig. 1(h) and Supplemental Material, Fig. S(1)] [29]. Because they are well separated, the charge state of each DB can be assigned reliably by a single line scan [Supplemental Material, Fig. S(3)] [29].

Interestingly, the occupation of DB structures observed at 0 V appears to depend strongly on Δz . Figure 2 compares a series of constant height line scan maps on a structure composed of six DBs with different Δz . The average occupation of each DB at each height can be inferred

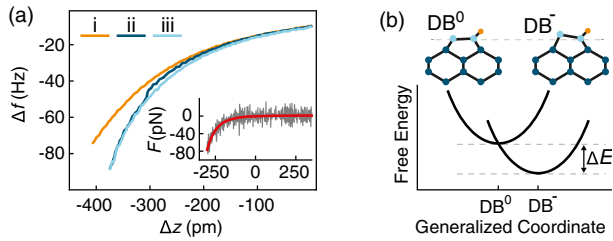


FIG. 3. Mechanically induced charge switching of a DB in a pair. (a) $\Delta f(z)$ at 0 V taken above a vacancy (i) and on a DB in a pair (ii—approach; iii—retract). Inset: the short range forces acting on the neutral DB [curve ii in (a)] up to the sharp step observed in $|\Delta f|$. See SM for more details. (b) Top panel: sketch of the equilibrium position of the host atom of a neutral DB (left) and a negatively charged DB (right). Dark blue, light blue, and orange atoms represent bulk silicon, silicon dimers, and hydrogen, respectively. Bottom panel: Free energy diagram depicting the neutral to negative charge transition for a DB due to the mechanical displacement of the host atom by the tip. ΔE corresponds to the lattice relaxation energy.

from the histograms of the Δf measured over each DB [Supplemental Material, Fig. S(3)] [29]. More simply, the average occupation of the entire structure can be inferred by counting the number of dark bars in each line scan map. At the tip's closest approach [−320 pm, top panel Fig. 2(b)] all six DBs appear negatively charged. Upon withdrawing the tip by just 50 pm [−270 pm, Fig. 2(b) bottom panel], only three DBs image as negatively charged. This change in the apparent time-averaged occupation of the structure does not vary linearly with Δz , but instead transitions sharply between −300 and −290 pm [Fig. 2(c)].

To understand this trend we performed distance-dependent Δf spectroscopy [$\Delta f(z)$] at 0 V on the individual DBs of a pair [Fig. 3(a), blue curves] and over a vacancy on the surface [Fig. 3(a), orange curve]. We began by withdrawing the tip 700 pm from the reference height [29] to effectively eliminate the forces between the tip and sample, and we subsequently walked the tip towards the sample to progressively reintroduce them. Until approximately $\Delta z = -100$ pm, all three curves are nearly identical, confirming that the long range forces (i.e., capacitive forces due to the contact potential difference, and van der Waals interaction between the large number of surface and tip atoms) are dominant [47–49]. Focusing on the approach curve obtained over the DB, at $\Delta z = -302 \pm 2$ pm there is a sudden increase in the $|\Delta f|$ (observed at $\Delta z = -301 \pm 2$ pm on the other DB). Crucially, this results in hysteresis between the approach and retract curves, with the $|\Delta f|$ measured in the latter remaining larger until approximately $\Delta z = -100$ pm. Because of the similarity between the step in the approach curve and those observed in $\Delta f(V)$ experiments [e.g., Fig. 1(d)] we attribute this phenomenon to the localization of the pair's charge to the DB beneath the tip. Two observations confirm this: if a step was observed in the $\Delta f(z)$ obtained over one DB, subsequent $\Delta f(z)$ curves taken

over the same DB did not demonstrate this behavior. Instead, both the approach and retract curves trace the curve with the greater $|\Delta f|$, indicating the DB remained charged. In contrast to this behavior, if a step was observed in the $\Delta f(z)$ obtained over one DB and the subsequent $\Delta f(z)$ was performed on the other, the hysteresis was consistently observed, indicating we caused the charge to switch sites.

Similar hysteresis in $\Delta f(z)$ curves has previously been observed on the hydrogen-free Si(100) surface [50]. In their case, the presence of sudden hysteretic steps corresponded directly to a toggling of the buckling direction of a single Si(100) dimer. The authors concluded that at small absolute tip heights, short range forces between the probe and sample resulted in a mechanically-induced deformation of the lattice. The same mechanism is at play in our experiments. One distinction of our work is that the mechanical deformation also corresponds to a change in the charge state of the surface atom. This can be understood by considering the equilibrium positions of the host silicon atom for a negative and a neutral DB, which as noted earlier, differ due to the relaxation of the lattice [sketch in top panel, Fig. 3(b)] [44–46]. Because the forces are all attractive at the height corresponding to the step in the approach curve, the surface atom is displaced towards the tip, causing the atom to rehybridize and adopt greater sp^3 character. Consequently, the total free energy of the negatively charged state is lowered with respect to the neutral state, leading to the charging of the DB beneath the tip [bottom panel, Fig. 3(b)].

Because a charge manipulation mechanism based upon the mechanical manipulation of individual atoms has not been reported before, the unsuitability of electrostatic mechanisms in accounting for the results of this study must be explained. First, we note that even though the experiments were performed at 0 V, there still exists a field due to the contact potential difference. Because the work function of the Si sample is smaller than that of the W tip, this field causes states near the surface to be raised in energy relative to the bulk (i.e., upward tip-induced band bending). This effect becomes stronger with decreasing tip-sample separation; as such, the DB (0/−) charge transition level remains above the bulk Fermi level, and consequently, tip-induced band bending cannot be used to explain the preferential charging of DBs beneath the tip. Screening of the local charges by the metallic tip was also considered and found to be incapable of accounting for the experimental observations [29]. Further evidence for a mechanical mechanism is found by isolating the forces acting between the tip and the DB from the total tip-sample interaction by using $\Delta f(z)$ curves obtained over dimer vacancies on the surface [Supplemental Material, Figs. S(4) and S(5)] [29] to separate the long and short range force contributions [47–49]. We found that the short range forces required to lift the equilibrium position of the neutral host atom are fit best by a function of the form $-C/z^7$, where z is

the absolute tip height and C is a constant [Supplemental Material, Fig. S(5)] [29]. This strongly suggests that van der Waals forces are responsible for displacing the host atom [51]. The functional form of the forces measured between the tip and the neutral and negatively charged DB [Supplemental Material, Fig. S(5)] also allow a charge manipulation mechanism based on an electrostatic shift of the DB (0/−) charge transition level by a charged atom on the tip’s apex to be ruled out with confidence [29]. A force of -75 ± 13 pN (-77 ± 12 pN) was found for the right (left) DB [inset Fig. 3(a)]. Sweetman *et al.* reported that a force in the range of 100–600 pN was required to toggle the Si dimer [50,52], and that this force corresponded to the formation of a covalent bond between the tip’s apex atom and the surface atom. The comparably small force reported here is consistent with the interpretation that van der Waals forces are responsible for lifting the silicon atom in our experiments.

The experiments in Fig. 2 can now be clearly explained. At small absolute tip heights, the short range forces are strong enough that as the probe scans over the structure the charging of each DB becomes favorable whenever it is beneath the tip [top panel, Fig. 2(b)]. This necessitates that electrons vacate prior negatively charged DBs such that the overall occupation of the structure remains constant. Upon withdrawing the tip a short distance, however, this effect is greatly diminished. As a result, specific charge configurations are observed to remain stable for many sequential measurements [>15 s on average, bottom panel, Fig. 2(b)]. Another crucial observation is that only two charge configurations appear consistently: the two outer DBs remain continuously charged and a single negative charge is observed to switch between the two central DBs, similar to the behavior observed on an isolated pair. By observing that the total amount of time the central charge spends in the left DB (50%) is roughly equal to the right (46%), and noting the structure’s symmetry, it is clear that these two charge configurations correspond to the degenerate ground state. Higher energy charge configurations were not observed for this structure, likely because the Coulombic interaction between closely spaced negative charges makes them energetically unfavorable, e.g., if DBs 1, 2, and 6 in Fig. 2(d) were negatively charged. We therefore identify two interaction regimes [Fig. 2(c)]: one where charge can be controllably manipulated by the tip (the *write regime*) and another where stable or metastable charge configurations can be observed (the *read regime*).

To further validate our assignment of the write and read regimes, we performed the experiments depicted in schemes Figs 4(a)–4(c) on the symmetric structure [Fig. 4(d)] and an asymmetric structure composed of five DBs [Fig. 4(h)]. First, we restricted the measurements to the read regime [schemes Figs. 4(a),4(e),4(i)], which allows us to characterize the intrinsic charge configurations of the structures and assess their relative energies based on how often they occur [histograms in Supplemental Material, Fig. S(6)] [29].

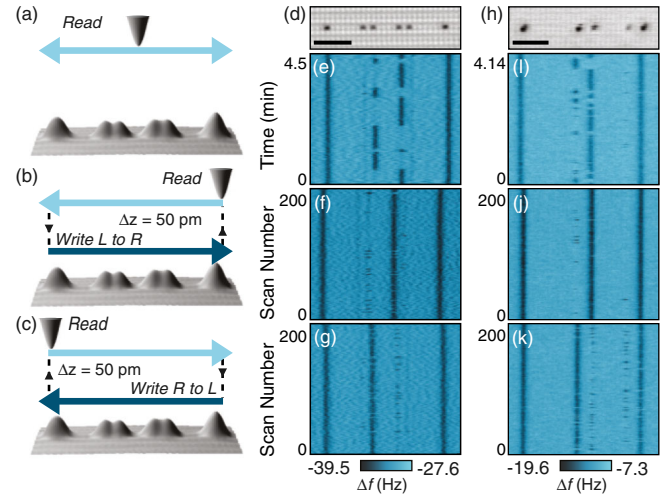


FIG. 4. Controlled preparation of charge configurations in symmetric and asymmetric DB structures. Visualization of the scan modes: (a) all measurements are restricted to the *read regime*; (b) The tip is scanned from left to right (*L to R*) in the *write regime*, retracted 50 pm to the read regime, and scanned back across; (c) the same process as (b) with directions reversed (*write R to L*). (d) Constant height Δf image of the symmetric six-DB structure (0 V, -300 pm). (e)–(g) Maps of 200 line scans across structure in (d) corresponding to scheme (a) shown in (e), scheme (b) shown in (f), and scheme (c) shown in (g) (*write regime*: -320 pm, *read regime*: -270 pm). (h) Constant height Δf image of the asymmetric five-DB structure, -350 pm, 0 V. (i)–(k) Maps of 200 line scans across structure (i) corresponding to scheme (a) (i), scheme (b) (j), and scheme (c) (k) (*write regime*: -370 pm, *read regime*: -320 pm). The scale bars in (d) and (h) are 3 nm. Data displayed in (e)–(k) correspond to the read regime of each sequence.

Subsequent experiments contained two associated phases: in the write phase, the tip was scanned across the structure at close proximity; in the read phase, the tip was retracted 50 pm with respect to the write phase and scanned back across [schemes Figs. 4(b),4(c)] to observe the prepared charge configuration. Indeed, Figs. 4(f),4(g) and 4(j),4(k) confirm that charge in the interior of both structures can be manipulated. On the symmetric structure, we could consistently initiate charge to the right [Fig. 4(f) 85%] or left [Fig. 4(g) 79%] central DB, corresponding to preparation of the degenerate ground state configurations observed in Fig. 4(e). On the asymmetric structure, measurements restricted to the read regime [Fig. 4(i)] demonstrate that this system has three negative charges. On this structure, only the charge confined to the inner pair fluctuates, but because the structure is asymmetric, these two charge configurations are nondegenerate. Although we expected the interior charge to favor the left DB of the pair, because that configuration would minimize the electrostatic interaction between the three negative charges, we observe the opposite [Fig. 4(i) 18% vs 73%, respectively]. This indicates that other charged species (e.g., DBs or ionized donors) likely act as an

additional electrostatic bias on this structure. We note, however, that hidden biases can be counteracted by patterning additional DBs in the area surrounding DB structures [Supplemental Material, Fig. S(7)] [29]. Using the techniques previously described the central charge could be manipulated to selectively occupy the right [Fig. 4(j) 92%] or left [Fig. 4(k) 67%] DB of the pair, demonstrating that in addition to the ground state configurations the occurrence of metastable charge configurations can also be enhanced [Fig. 4(i)].

These results demonstrate that single electrons can be manipulated within structures derived from DBs by using the probe to mechanically manipulate the equilibrium position of the host atoms. Underlying this charge control mechanism is relaxation of the silicon lattice, which acts to stabilize negatively charged DBs. The techniques presented here expand the scanning probe toolkit with the ability to position charge within atomic structures to prepare desired charge configurations.

We would like to thank Mark Salomons and Martin Cloutier for their technical expertise. We also thank Leo Gross and Gerhard Meyer for stimulating discussions. We thank NRC, NSERC, and AITF for their financial support.

M. R., W. V., and T. D. contributed equally to this work.

*rashidi@ualberta.net

†Current address: Centre for Quantum Computation and Communication Technologies, School of Electrical Engineering and Telecommunications, UNSW, Sydney, New South Wales 2052, Australia.

wyattvine@gmail.com

‡thdienel@gmail.com

- [1] D. K. Schweizer and E. K. Eigler, *Nature (London)* **344**, 524 (1990).
- [2] Y. Sugimoto, P. Pou, O. Custance, P. Jelinek, M. Abe, R. Perez, and S. Morita, *Science* **322**, 413 (2008).
- [3] M. R. Slot, T. S. Gardenier, P. H. Jacobse, G. C. P. van Miert, S. N. Kempkes, S. J. M. Zevenhuizen, C. M. Smith, D. Vanmaekelbergh, and I. Swart, *Nat. Phys.* **13**, 672 (2017).
- [4] R. Drost, T. Ojanen, A. Harju, and P. Liljeroth, *Nat. Phys.* **13**, 668 (2017).
- [5] S. Fölsch, J. Martínez-Blanco, J. Yang, K. Kanisawa, and S. C. Erwin, *Nat. Nanotechnol.* **9**, 505 (2014).
- [6] A. A. Khajetoorians, J. Wiebe, B. Chilian, and R. Wiesendanger, *Science* **332**, 1062 (2011).
- [7] M. Fuechsle, J. A. Miwa, S. Mahapatra, H. Ryu, S. Lee, O. Warschkow, L. C. L. Hollenberg, G. Klimeck, and M. Y. Simmons, *Nat. Nanotechnol.* **7**, 242 (2012).
- [8] F. E. Kalf, M. P. Rebergen, E. Fahrenfort, J. Girovsky, R. Toskovic, J. L. Lado, J. Fernández-Rossier, and A. F. Otte, *Nat. Nanotechnol.* **11**, 926 (2016).
- [9] T. Huff, H. Labidi, M. Rashidi, R. Achal, L. Livadaru, T. Dienel, J. Pitters, and R. A. Wolkow, *arXiv:1706.07427*.
- [10] J. Repp, G. Meyer, F. E. Olsson, and M. Persson, *Science* **305**, 493 (2004).
- [11] G. V. Nazin, X. H. Qiu, and W. Ho, *Phys. Rev. Lett.* **95**, 166103 (2005).
- [12] L. Gross, F. Mohn, P. Liljeroth, J. Repp, F. J. Giessibl, and G. Meyer, *Science* **324**, 1428 (2009).
- [13] M. Sterrer, T. Risse, U. M. Pozzoni, L. Giordano, M. Heyde, H. P. Rust, G. Pacchioni, and H. J. Freund, *Phys. Rev. Lett.* **98**, 096107 (2007).
- [14] T. Leoni, O. Guillermet, H. Walch, V. Langlais, A. Scheuermann, J. Bonvoisin, and S. Gauthier, *Phys. Rev. Lett.* **106**, 216103 (2011).
- [15] W. Steurer, J. Repp, L. Gross, I. Scivetti, M. Persson, and G. Meyer, *Phys. Rev. Lett.* **114**, 036801 (2015).
- [16] W. Steurer, S. Fatayer, L. Gross, and G. Meyer, *Nat. Commun.* **6**, 8353 (2015).
- [17] S. D. Bennett, L. Cockins, Y. Miyahara, P. Grutter, and A. A. Clerk, *Phys. Rev. Lett.* **104**, 017203 (2010).
- [18] K. Teichmann, M. Wenderoth, S. Loth, J. K. Garleff, A. P. Wijnheijmer, P. M. Koenraad, and R. G. Ulbrich, *Nano Lett.* **11**, 3538 (2011).
- [19] M. Setvin, J. Hulva, G. S. Parkinson, M. Schmid, and U. Diebold, *Proc. Natl. Acad. Sci. U.S.A.* **114**, E2556 (2017).
- [20] S. Fatayer, B. Schuler, W. Steurer, I. Scivetti, J. Repp, L. Gross, M. Persson, and G. Meyer, *Nat. Nanotechnol.* **13**, 376 (2018).
- [21] M. B. Haider, J. L. Pitters, G. A. DiLabio, L. Livadaru, J. Y. Mutus, and R. A. Wolkow, *Phys. Rev. Lett.* **102**, 046805 (2009).
- [22] L. Liu, T. Dienel, R. Widmer, and O. Gröning, *ACS Nano* **9**, 10125 (2015).
- [23] F. Schulz, M. Ijäs, R. Drost, S. K. Hämäläinen, A. Harju, A. P. Seitsonen, and P. Liljeroth, *Nat. Phys.* **11**, 229 (2015).
- [24] N. Pavliček, Z. Majzik, G. Meyer, and L. Gross, *Appl. Phys. Lett.* **111**, 053104 (2017).
- [25] T. R. Huff, H. Labidi, M. Rashidi, M. Koleini, R. Achal, M. H. Salomons, and R. A. Wolkow, *ACS Nano* **11**, 8636 (2017).
- [26] R. Achal, M. Rashidi, J. F. Croshaw, D. Churchill, M. Taucer, T. Huff, M. Cloutier, J. Pitters, and R. A. Wolkow, *Nat. Commun.* **9**, 2778 (2018).
- [27] M. Rashidi, E. Lloyd, T. R. Huff, R. Achal, M. Taucer, J. J. Croshaw, and R. A. Wolkow, *ACS Nano* **11**, 11732 (2017).
- [28] M. Taucer, L. Livadaru, P. G. Piva, R. Achal, H. Labidi, J. L. Pitters, and R. A. Wolkow, *Phys. Rev. Lett.* **112**, 256801 (2014).
- [29] See Supplemental Material at <http://link.aps.org/supplemental/10.1103/PhysRevLett.121.166801>, which includes Refs. [25,30–40], for methods, definition and discussion of error rate, data processing for repeated line scan experiments and assignment of digital charge configurations, height-dependent contrast in Δf images, frequency to force conversion, discussion of charge manipulation mechanisms based on electrostatics, as well as additional experimental data.
- [30] F. J. Giessibl, *Appl. Phys. Lett.* **76**, 1470 (2000).
- [31] J. E. Sader and S. P. Jarvis, *Appl. Phys. Lett.* **84**, 1801 (2004).
- [32] J. Welker, E. Illek, and F. J. Giessibl, *Beilstein J. Nanotechnol.* **3**, 238 (2012).
- [33] M. Rezeq, J. Pitters, and R. Wolkow, *J. Chem. Phys.* **124**, 204716 (2006).
- [34] H. Labidi, M. Koleini, T. Huff, M. Salomons, M. Cloutier, J. Pitters, and R. A. Wolkow, *Nat. Commun.* **8**, 14222 (2017).

- [35] S. Jarvis, A. Sweetman, J. Bamidele, L. Kantorovich, and P. Moriarty, *Phys. Rev. B* **85**, 235305 (2012).
- [36] J. L. Pitters, P. G. Piva, and R. A. Wolkow, *J. Vac. Sci. Technol., B* **30**, 021806 (2012).
- [37] M. Rashidi, J. A. J. Burgess, M. Taucer, R. Achal, J. L. Pitters, S. Loth, and R. A. Wolkow, *Nat. Commun.* **7**, 13258 (2016).
- [38] J. W. Lyding, T. C. Shen, J. S. Hubacek, J. R. Tucker, and G. C. Abeln, *Appl. Phys. Lett.* **64**, 2010 (1994).
- [39] S. R. Schofield, N. J. Curson, J. L. O'Brien, M. Y. Simmons, R. G. Clark, N. A. Marks, H. F. Wilson, G. W. Brown, and M. E. Hawley, *Phys. Rev. B* **69**, 085312 (2004).
- [40] N. J. Curson, S. R. Schofield, M. Y. Simmons, L. Oberbeck, J. L. O'Brien, and R. G. Clark, *Phys. Rev. B* **69**, 195303 (2004).
- [41] L. Livadaru, P. Xue, Z. Shaterzadeh-Yazdi, G. A. DiLabio, J. Mutus, J. L. Pitters, B. C. Sanders, and R. A. Wolkow, *New J. Phys.* **12**, 083018 (2010).
- [42] Z. Shaterzadeh-Yazdi, B. C. Sanders, and G. A. DiLabio, *J. Chem. Phys.* **148**, 154701 (2018).
- [43] F. E. Olsson, S. Paavilainen, M. Persson, J. Repp, and G. Meyer, *Phys. Rev. Lett.* **98**, 176803 (2007).
- [44] J. E. Northrup, *Phys. Rev. B* **40**, 5875 (1989).
- [45] S. R. Schofield, P. Studer, C. F. Hirjibehedin, N. J. Curson, G. Aepli, and D. R. Bowler, *Nat. Commun.* **4**, 1649 (2013).
- [46] H. Kawai, O. Neucheva, T. Leh, C. Joachim, and M. Saeys, *Surf. Sci.* **645**, 88 (2016).
- [47] M. A. Lantz, H. J. Hug, R. Hoffmann, P. J. A. van Schendel, P. Kappenberger, S. Martin, A. Baratoff, and H.-J. Güntherodt, *Science* **291**, 2580 (2001).
- [48] M. Ternes, C. González, C. P. Lutz, P. Hapala, F. J. Giessibl, P. Jelínek, and A. J. Heinrich, *Phys. Rev. Lett.* **106**, 016802 (2011).
- [49] A. Sweetman and A. Stannard, *Beilstein J. Nanotechnol.* **5**, 386 (2014).
- [50] A. Sweetman, S. Jarvis, R. Danza, J. Bamidele, S. Gangopadhyay, G. A. Shaw, L. Kantorovich, and P. Moriarty, *Phys. Rev. Lett.* **106**, 136101 (2011).
- [51] F. Bocquet, L. Nony, and C. Loppacher, *Phys. Rev. B* **83**, 035411 (2011).
- [52] S. Jarvis, A. Sweetman, J. Bamidele, L. Kantorovich, and P. Moriarty, *Phys. Rev. B* **85**, 235305 (2012).